Available online at www.sciencedirect.com
ScienceDirect
Acta Materialia 57 (2009) 4102–4108
Acta MATERIALIA
www.elsevier.com/locate/actamat

First principles impurity diffusion coefficients

M. Mantina [a,*], Y. Wang [a], L.Q. Chen [a], Z.K. Liu [a], C. Wolverton [b]

[a] Department of Materials Science and Engineering, The Pennsylvania State University, University Park, PA 16802, USA
[b] Department of Materials Science and Engineering, Northwestern University, Evanston, IL 60208, USA

Received 10 April 2009; accepted 4 May 2009
Available online 22 June 2009

Abstract

We report the prediction of impurity diffusion coefficients entirely from first principles, using density-functional theory (DFT) calculations. From DFT we obtain all microscopic parameters in the pre-factor and activation energy of impurity diffusion coefficients: (i) the correlation factor through a five frequency model, (ii) the impurity jump frequency within the framework of transition state theory and (iii) the free energies of vacancy formation and vacancy–solute binding. Specifically, we calculate the impurity diffusion coefficients of Mg, Si and Cu in dilute face-centered cubic Al alloys. The results show excellent agreement with experimental data. We discuss the factors contributing to the trends in diffusivities of these impurities.
Published by Elsevier Ltd. on behalf of Acta Materialia Inc.

Keywords: Tracer diffusion of Mg, Si, Cu; Activation energy and diffusion pre-factor; Dilute aluminum alloys; Density-functional theory

1. Introduction

During the past two decades there have been many efforts to determine diffusion coefficients using fundamental electronic/atomistic approaches [1–8]. The calculations have been either from empirical or semi-empirical approaches [1,8] or involved approximations for the values of certain quantities [2–7]. Recently we presented [9] a parameter-free first principles procedure to predict vacancy-mediated self-diffusion coefficients in cubic systems within the framework of transition state theory (TST). Here we extend this first principles approach to the case of impurity diffusion in face-centered cubic (fcc) systems using the five frequency model developed by LeClaire and Lidiard [10].

The five frequency model has been previously employed to determine impurity diffusion coefficients in alloys using atomistic/electronic structure calculations. For example, Adams et al. [1] predicted impurity diffusion coefficients in fcc metals using lattice static calculations with embedded atom potentials. Janotti et al. [5] and Kremar et al. [6] predicted diffusion coefficients of transition elements in fcc Ni via first principles calculations. In these studies the diffusion pre-factors were not explicitly calculated, but approximated to be the same for all solute elements. Recently Simonovic and Sluiter [11] conducted an extensive, systematic study of first principles activation energies in Al across a wide range of impurities. There have also been a number of attempts [6,12–16] to elucidate the trends in solute diffusion coefficients based on factors such as size, valence or solubility of the impurity in the host lattice. In most cases the analysis was mainly based on the relative values of activation energies for diffusion of impurities/solutes.

In the present work we use a first principles approach to calculate both the diffusion pre-factor (D_0) and the activation energy (Q) of impurity diffusion, including the important contributions of correlation for impurity diffusion. Our first principles calculations include both atomically relaxed static total energies, as well as direct force constant phonon frequencies and vibrational free energies. We consider the well-studied cases of impurity diffusion of Mg, Si and Cu in fcc Al. We examine the trends in solute diffusivities based on both D_0 and Q. This paper is organized as follows. In Section 2 the basic atomic theory of impurity diffusion is presented and in Section 3 the methodology

* Corresponding author.
E-mail address: manjeera.m@gmail.com (M. Mantina).

1359-6454/$36.00 Published by Elsevier Ltd. on behalf of Acta Materialia Inc.
doi:10.1016/j.actamat.2009.05.006

to compute the microscopic quantities in the five frequency model is detailed. The results and discussion are presented in Sections 4 and 5, respectively.

2. Equations for impurity diffusion coefficients

Impurities in fcc metals diffuse predominantly via a vacancy mechanism [17]. To describe impurity diffusion one must of course consider the jump frequency of the impurity atom into a neighboring vacant site. However, in addition, the situation is complicated by the fact that in the presence of an impurity the jump frequencies of host atoms surrounding the impurity are different compared with that in the pure element system, and one must consider each of these distinct atomic jumps to describe impurity diffusion with its correlation factor. Le Claire and Lidiard [10] described diffusion in dilute fcc alloys with dilute vacancy concentration in terms of five jump frequencies as:

$$\frac{D_2}{D_0} = \frac{f_2}{f_0}\frac{w_4}{w_0}\frac{w_1}{w_3}\frac{w_2}{w_1} \tag{1}$$

In this equation D_2 is the diffusion coefficient of the impurity atom in the host lattice, D_0 is the self-diffusion coefficient of the pure host element, f_2 is the correlation factor for impurity diffusion, f_0 is the self-diffusion correlation factor and w_j ($j = 0 - 4$) are the five jump frequencies as illustrated in Fig. 1. w_0 is the host atom jump in the absence of an impurity, w_1 is the jump for a host atom (nearest neighbor to an impurity) jump which does not "dissociate" the impurity from the vacancy, w_2 is the impurity atom jump, w_3 is the host atom jump which "dissociates" the impurity and vacancy and w_4 is the reverse of jump w_3, i.e. the host atom jump that "associates" the impurity and vacancy.

The impurity diffusion correlation factor, f_2, is related to the probability of the impurity atom making a reverse jump back to its previous position. It includes the probability (function F) of the vacancy returning to its position after disassociation by a w_3 jump, and is given by Le Claire [18] in terms of the jump frequencies via the following expression:

$$f_2 = \frac{1 + 3.5(w_3/w_1)F(w_4/w_0)}{1 + (w_2/w_1) + 3.5(w_3/w_1)F(w_4/w_0)}. \tag{2}$$

By explicitly considering the probabilities of the vacancy returning from second, third and fourth nearest neighboring positions to its original position, F was defined by Manning [19] as:

$$F(x) = 1 - \frac{10x^4 + 180.5x^3 + 927x^2 + 1341}{7(2x^4 + 40.2x^3 + 254x^2 + 597x + 435)}, \tag{3}$$

where x is w_4/w_0.

Based on transition state theory (TST), the atom jump frequency is written as [20];

$$w = v^* \exp(-\Delta H_m/k_B T), \tag{4}$$

where ΔH_m is the change in enthalpy of the system between the state in which the diffusing atom is in its initial equilibrium lattice position (hereafter referred to as the initial state) and the state in which it is at the saddle point along the diffusion path (hereafter referred to as the transition state), and v^* is the effective frequency described by Vineyard [21] as the quotient of the product of vibrational frequencies of the initial state v_i to that of the non-imaginary frequencies of the transition state v_i'. For a system with N vibrational degrees of freedom v^* is given by:

$$v^* = \frac{\prod_{i=1}^{N} v_i}{\prod_{i=1}^{N-1} v_i'}. \tag{5}$$

As illustrated in Fig. 1, three types of w_3 and w_4 jumps are possible in an fcc lattice, depending on whether the second, third or fourth nearest neighboring site to the impurity is involved in the jump process. The five frequency model assumes that the three types of each jump are equiv-

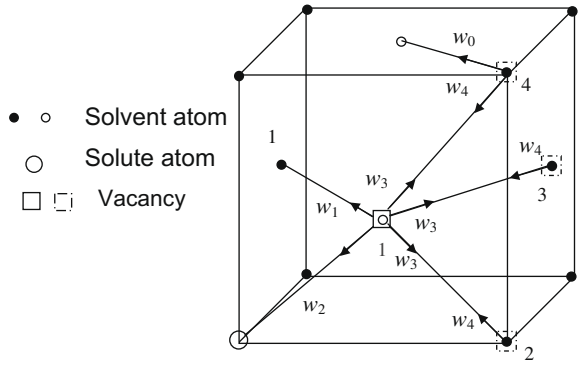

Fig. 1. Five frequency model illustration for the case of an fcc system with a dilute impurity concentration. The arrows indicate the direction of the vacancy jump and the numbers n stand for the nth nearest neighboring site to the impurity. For the cases of w_1, w_2 and w_3 jumps the vacancy position adjacent to the solute is indicated by a solid box and filled circles indicate solvent atoms that make these jumps. For jumps w_0 and w_4 the vacancy position away from the solute is indicated by a dotted box and the solvent positions for these jumps are indicated by open circles.

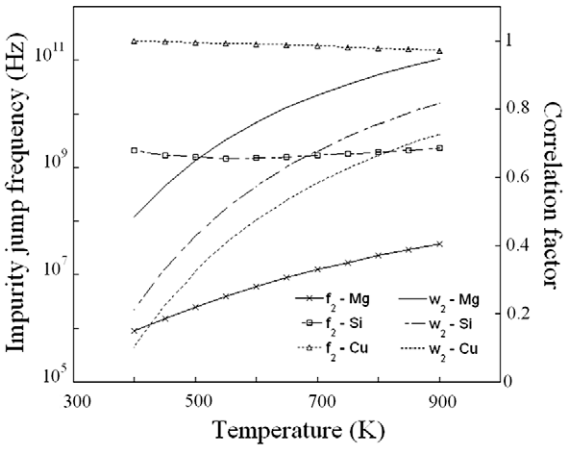

Fig. 2. Impurity jump frequency and correlation factor as a function of temperature of Mg, Si and Cu in Al from LDA.

alent and thus have the same jump frequencies. In addition, w_3 is simply the reverse of w_4 and hence these two jumps have the same transition state, resulting in the expression [22]:

$$\frac{w_4}{w_3} = \exp\left(\frac{\Delta G_b}{k_B T}\right), \tag{6}$$

where ΔG_b is the solute–vacancy binding free energy representing the free energy difference between the state where solute and vacancy are nearest neighbors (initial state of w_3 and final state of w_4) and the state where they are separate (initial state of w_4 and final state of w_3).

Eq. (1) is a valid description of the impurity diffusion coefficient in an fcc system with a dilute impurity concentration. However, it is often convenient to represent this equation in an Arrhenius form to obtain the pre-factor and activation energy of impurity diffusion. Combining the expression describing the self-diffusion coefficient [9],

$$D_0 = f_0 w_0 C_0 a^2 \quad \text{with } C_0 = \exp\left(-\frac{\Delta G_f^{\circ}}{k_B T}\right),$$

with Eq. (6) we can write Eq. (1) as:

$$D_2 = f_2 w_2 a^2 \exp\left(-\frac{\Delta G_f^{\circ} - \Delta G_b}{k_B T}\right), \tag{7}$$

where a is the lattice parameter and ΔG_f° is the free energy of vacancy formation in the pure host system. Representing $\Delta G_f^{\circ} - \Delta G_b$ as ΔG_f, the free energy for vacancy formation minus the solute–vacancy binding [18], along with the associated enthalpy and entropy, ΔH_f and ΔS_f, and substituting $w_2 = v^* \exp(-\Delta H_m / k_B T)$, the impurity diffusion Eq. (7) can be expressed in an Arrhenius form as [22]:

$$D_2 = \frac{f_2 a^2 v^* \exp\left(\frac{\Delta S_f}{k_B}\right)}{\exp\left(\frac{k_B d \ln f_2 / d(1/T)}{k_B T}\right)} \times \exp\left(-\frac{(\Delta H_f + \Delta H_m - k_B d \ln f_2 / d(1/T))}{k_B T}\right), \tag{8}$$

where the activation energy is given by

$$Q = \Delta H_f + \Delta H_m - k_B d \ln f_2 / d(1/T)$$

and the diffusion pre-factor is

$$D_o = \frac{f_2 a^2 v^* \exp\left(\frac{\Delta S_f}{k_B}\right)}{\exp\left(\frac{k_B d \ln f_2 / d(1/T)}{k_B T}\right)}.$$

We note that the temperature dependence of f_2 from Eq. (4) contributes to the activation energy of impurity diffusion.

3. Methodology

For the first principles calculations we use the Vienna ab initio simulation package ||VASP| [23] with projector augmented wave (PAW) potentials [24,25]. The potentials used for each of the elements Al, Mg, Si and Cu do not treat any semi-core states as valence. We have compared results using both the local density approximation (LDA) [26] and the generalized gradient approximation (GGA) [27] for the exchange correlation. Convergence tests indicate that a Monkhorst–Pack k point mesh of $11 \times 11 \times 11$ and an energy cut-off of 300 eV are suitable to yield converged impurity migration barriers within 0.01 eV. Similar convergence of the energetics is obtained in tests using supercells with 32 and 64 lattice sites. Hence, we employ supercells with 32 lattice sites ($2 \times 2 \times 2$ conventional fcc cells), replacing one host atom with an impurity atom.

The thermodynamic properties of the initial and transition states of a jump need to be determined to calculate its jump frequency (w_j) using Eq. (4). Each initial state is completely relaxed with respect to internal coordinates, volume and shape. We quantitatively determine the transition state with the saddle point along the minimum energy diffusion path by nudged elastic band (NEB) [28] calculations. We first tested an eight image versus single image NEB calculation for the w_0 jump, and finding good agreement for these relatively high symmetry jumps we performed simply single image calculations for the other jumps. Conducting NEB calculations is specifically important for the case of jumps w_1, w_3 and w_4 with asymmetry between the initial and final states. (For the jumps w_0 and w_2 the initial and final states are equivalent and hence there is high symmetry in the jump geometry. Hence, NEB results often give the obvious guess, i.e. the center point between the initial and final positions of the diffusing atom.) Three of the jumps, w_1, w_2 and w_3, have the same initial state, with the vacancy adjacent to the impurity atom, and two jumps, w_3 and w_4, have the same transition state since they represent the same atomic jump, just in opposite directions. For the w_1 jump both the initial and transition states of the jump in the pure host system need to be considered.

Phonon frequencies are calculated using the direct force constant supercell approach [29] as implemented in the Alloy Theoretic Automated Toolkit (ATAT) [30] package. The same energy cut-off and k point mesh size as for total energy calculations are used for the vibrational calculations. We obtain v^* from Eq. (5) using phonon frequencies from the Γ point wave vector. It has been observed in our previous work [9] that anharmonic effects from volume expansion are negligible for aluminum. Hence, in the present work we adopt the harmonic approximation (HA). The migration barrier is then obtained as the difference between the energies of the relaxed configurations at 0 K (E_c) of the initial and transition states of a jump. There exists an error in the energetics of vacancy-containing systems obtained from density-functional theory due to an overestimation of the energy of the vacancy, which may be viewed as an internal "surface" [31]. This surface error is seen to be smaller for LDA than for GGA [32] due to cancellation of errors within the exchange and correlation functions of the total energy [33]. Corrections for this error (referred to as the surface correction) for the different jumps in an

impurity containing system are not available in the literature. We use the computed migration barriers directly without any correction along with the vibrational pre-factors to obtain the jump frequencies and, subsequently, the impurity correlation factor.

Knowledge of the self-diffusion coefficient along with the calculated five jump frequencies and the impurity diffusion correlation factor allows one to obtain the impurity diffusion coefficient using Eq. (1). We use our first principles calculated Al self-diffusion coefficient [34] (without surface correction) to obtain the impurity diffusion coefficient in Al, illustrated in Figs. 3–6. In order to obtain the individual diffusion parameters, i.e. the diffusion pre-factor and the activation energy (Eq. (8)), the enthalpy and entropy of vacancy formation in pure Al and the enthalpy and entropy of vacancy–solute binding are calculated following standard thermodynamic relations [35] from the respective free energy expressions:

$$\Delta G_f^{\circ} = G_{PS} - \left(\frac{N-1}{N}\right) G_{IS}^{w0}, \qquad \Delta G_b = -(G_{IS}^{w3} - G_{IS}^{w4}) \tag{9}$$

where G_{PS} is the free energy of the system without any vacancies and G_{IS}^{w0}, G_{IS}^{w3} and G_{IS}^{w4} are the free energies of

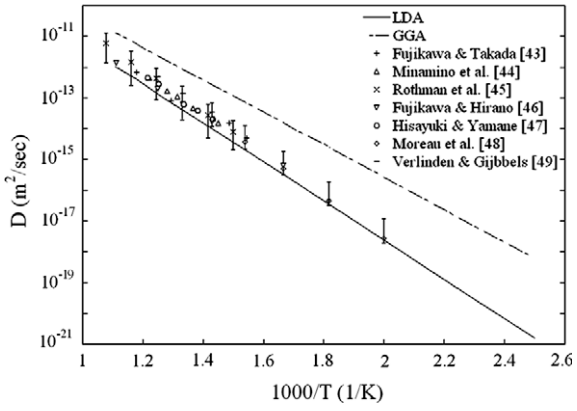

Fig. 3. Diffusion coefficient of Mg in fcc Al, comparing results from LDA and GGA with experimental data [43–49].

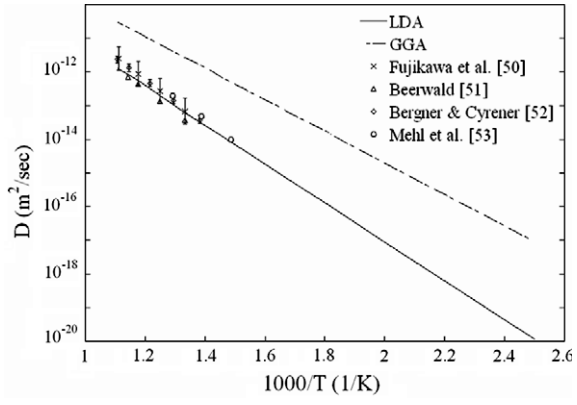

Fig. 4. Diffusion coefficient of silicon in fcc Al, comparing results from LDA and GGA with experimental data [50–53].

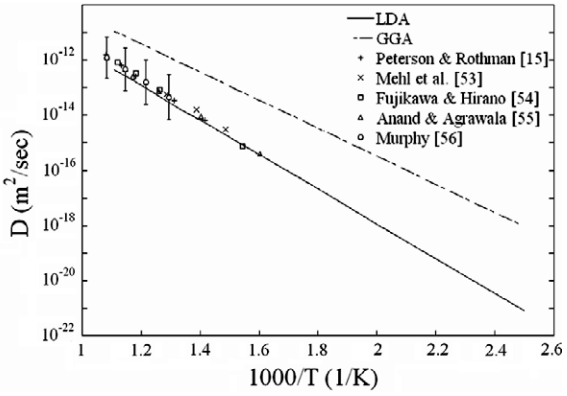

Fig. 5. Diffusion coefficient of copper in fcc Al, comparing results from LDA and GGA with experimental data [15,53–56].

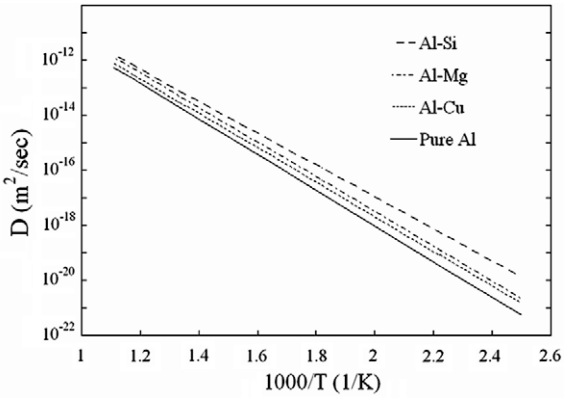

Fig. 6. Calculated diffusion coefficients of the impurities Mg, Si and Cu in Al in comparison with Al self-diffusion [9].

the initial states of the system for w_0, w_3 and w_4 jumps, respectively. Again, no surface correction is added to the energetics of these states with vacancy. The free energies are calculated from the total energies (E_c) and the vibrational frequencies, following the harmonic approximation [36]:

$$G(T) = E_c + k_B T \sum_q \sum_j \ln\left\{2\sinh\left[\frac{h\nu_j(q)}{2k_B T}\right]\right\}, \tag{10}$$

where the summation j is over the vibrational frequencies at each wave vector q.

4. Results and discussion

Table 1 illustrates our calculated enthalpy and entropy of vacancy formation ($\Delta H_f^{\circ}, \Delta S_f^{\circ}$) and migration barrier (ΔH_m°) in pure Al, as well as the enthalpy and entropy of solute–vacancy binding (ΔH_b, ΔS_b) and migration barrier (ΔH_m) of Mg, Si and Cu in Al. Where available, these quantities are compared with experimental measurements. We find a good agreement between our first principles calculated energetics and experimentally measured quantities. Our solute–vacancy binding energies (Table 1) also compare very well

Table 1
Calculated enthalpy and entropy of solute–vacancy binding (ΔH_b, ΔS_b) and solute migration barrier (ΔH_m) in system with impurity, and enthalpy and entropy of vacancy formation (ΔH_f°, ΔS_f°) and migration barrier (ΔH_m°) in pure system, from LDA and GGA (without surface correction) in comparison with experimental data. Experimental migration barriers are deduced from activation energy and enthalpy of vacancy formation of the indicated references, assuming effect of correlation to be zero.

System	Enthalpy (eV) ΔH_f° or ΔH_b			Entropy (k_B) ΔS_f° or ΔS_b			Migration barrier (eV) ΔH_m° or ΔH_m		
	LDA	GGA	Experimental	LDA	GGA	Experimental	LDA	GGA	Experimental
Al	0.71	0.55	0.67 ± 0.03 [57]	1.21	1.18	1.10 [57]	0.58	0.52	0.59 ± 0.03 [15]
Al–Mg	−0.07	−0.08	-0.01 ± 0.04 [38]	−0.27	−0.32	-0.10 ± 0.50 [38]	0.42	0.38	0.67 ± 0.07 [45]
Al–Si	0.11	0.10	0.03 [38]	0.44	0.33	−2.00 [38]	0.55	0.479	0.64 ± 0.03 [52]
Al–Cu	0.03	0.01	±0.12 [38]	0.16	−0.51	±1.50 [38]	0.57	0.476	0.73 ± 0.15 [15]

with the previous first principles work of Wolverton [37], who used 64 atom supercells. We also report solute–vacancy binding entropies, however, there is a discrepancy with experimental data for these binding entropies. We suspect that this discrepancy may be due to the use of non-equilibrium quenching methods to obtain the experimental values of binding entropies, as discussed by Balluffi and Ho [38]. From Table 1 it can also be seen that the energetics of vacancy formation and atom migration in pure and impurity containing systems from LDA show better agreement with experimental data than those from GGA. Thus the results from the current work strongly support the conclusion from previous studies [32,33] that LDA has a smaller surface correction error than GGA.

The LDA calculated results for different jumps are given in Tables 2–4 for Mg, Si, and Cu impurities in Al and the impurity jump frequencies with respect to temperature are plotted in Fig. 2. It can be seen from these data that the lowest jump frequency (w_2) of Cu in Al arises from the low ν^* and high ΔH_m Similarly, the highest jump frequency of Mg in Al comes from the high ν^* and low ΔH_m. Further, from Eq. (2) we note that the greater the frequency of the impurity jump w_2 and the lower the frequencies of jumps w_1 and w_3, the lower the resulting impurity diffusion correlation factor, indicating a highly correlated motion of the impurity atom. This behavior is clearly reflected in the data tabulated in Table 4.

The various correlation factors are also plotted in Fig. 2 as a function of temperature. The Cu and Si diffusion correlation factors are nearly constant, while the Mg diffusion correlation factor increases with temperature. This temperature dependence effectively contributes a value of 0.068 eV to the activation energy of Mg diffusion in Al through the $-k_B d \ln f_2/d(1/T)$ term in Eq. (8). The diffusion pre-factor (D_o) and activation energy (Q) are listed in Table 5, showing that there is a positive correlation between the size of the pre-factor and the size of the activation energy, specifically $D_{o-\mathrm{Mg}} > D_{o-\mathrm{Cu}} > D_{o-\mathrm{Si}}$ and $Q_{\mathrm{Mg}} > Q_{\mathrm{Cu}} > Q_{\mathrm{Si}}$. This correlation is an example of the ubiquitous Meyer–Neldel compensation law [39] which is observed in many thermal activated Arrhenius-type processes. According to this law the diffusion coefficient of solutes with greater activation barriers is compensated by an increased diffusion pre-factor.

Table 2
Calculated migration barriers ΔH_m (eV) of the five jumps of different impurities from LDA.

Impurity	w_0	w_1	w_2	w_3	w_4
Mg	0.58	0.68	0.42	0.50	0.57
Si	0.58	0.52	0.55	0.66	0.55
Cu	0.58	0.38	0.57	0.61	0.59

Table 3
Calculated ν^* (THz) for the five jumps of different impurities from LDA.

Impurity	w_0	w_1	w_2	w_3	w_4
Mg	16.6	21.8	18.6	13.3	17.1
Si	16.6	10.9	15.7	22.3	13.7
Cu	16.6	13.6	10.9	32.6	50.7

Our first principles calculated impurity diffusion coefficients are shown in Figs. 3–5. We find that the diffusion results from LDA are in excellent agreement with the experimental data. It should be noted that although the computed diffusion coefficients match well with experiments, there are discrepancies in the values of activation energy and diffusion pre-factor, as can be seen in Table 5. It has also been previously observed [11,40] that experimental activation barriers are consistently high compared with computational results. One possible reason for this discrepancy could be the experimental D_o and Q values being evaluated in small temperature ranges at high temperatures. However, further investigation of this discrepancy is warranted.

All of the calculated impurity diffusion coefficients for Si, Mg, and Cu in Al are plotted together in Fig. 6. From this figure we see a clear trend in diffusivities: $D_{\mathrm{Si}} > D_{\mathrm{Mg}} > D_{\mathrm{Cu}}$. We wish to understand this trend. Prior studies [6,12–16] have described trends in solute diffusivity in terms of the solute atomic size and its excess valence or its solubility in the host element. However, these simple characteristics alone do not lend themselves to a simple explanation for our results: Si, the fastest diffuser of the three impurities, has an atomic radius (r) intermediate between Mg and Cu [41]:

$$r_{\mathrm{Mg}}(1.597\mathrm{A})^\circ > r_{\mathrm{Si}}(1.392\mathrm{A})^\circ > r_{\mathrm{Cu}}(1.284\mathrm{A})^\circ.$$

Also, Cu, the slowest diffuser of the three, has a solubility (s) in Al intermediate between Mg and Si:

$$S_{\mathrm{Mg}} > S_{\mathrm{Cu}} > S_{\mathrm{Si}}$$

Table 4
Calculated five jump frequencies (Hz) and correlation factors for impurities diffusion along with jump frequency ratios entering Eq. (1). Results listed are for $T = 400$ K using ΔH_m from Table 2 and v^* from Table 3.

Impurity	w_0	w_1	w_2	w_3	w_4	f_2	w_4/w_0	w_1/w_3	w_2/w_1
Mg	8.31e5	5.81e4	9.18e7	6.60e6	1.09e6	0.16	1.3	0.01	1580
Si	8.31e5	3.35e6	1.86e6	1.24e5	1.76e6	0.66	2.1	27.02	0.56
Cu	8.31e5	2.39e8	7.17e5	6.72e5	1.87e6	0.99	2.2	354.98	0.003

Table 5
Diffusion pre-factor and activation energy from current LDA calculations to data in comparison with experiments and other theoretical calculations along with the assessed data by Du et al. [58]. For comparison, D_0 is 6.6e−6 and Q is 1.29 for pure Al [9].

System property		Present	Experimental data	Other computations
D_0 (m^2/sec)	Mg	1.19e−5	6.23e−6 [46] 1.24e−4 ± 0.22e−4 [45] 1e−4 [48] 6.6e−5 ± 1.7e−5 [49] 1.49e−5 [58]	1.24e−4 [1]
	Si	3.66e−6	2e−4 ± 0.66e−4 [43] 3.1e−5 [51] 3.5e−5 ± 5e−6 [52] 1.38e−5 [58]	3.46e−5 [1]
	Cu	4.37e−6	6.47e−5 [15] 2.9e−5 [56] 4.44e−5 [58]	6.5e−5 [1]
Q (eV)	Mg	1.27	1.19 [46] 1.35 ± 0.05 [48] 1.29 ± 0.015 [49] 1.25 [58]	1.35 [1] 1.2 [40] 1.13 [11]
	Si	1.15	1.41 ± 0.03 [43] 1.33 [51] 1.28 [52] 1.22 [58]	1.28 [1] 1.0 [40] 1.15 [11]
	Cu	1.25	1.4 ± 0.01 [15] 1.35 ± 0.07 [56] 1.39 [58]	1.4 [1] 1.18 [11]

for temperatures just below the melting point of Al [42]. Trends in diffusivities have often been correlated with the trends in activation energies or even migration barriers [6,12,13,15]. However, we see that these simple descriptors do not even provide a qualitative explanation of the diffusion coefficients: Mg has a higher activation barrier than Cu and yet has a higher diffusivity than Cu; also, Mg has a lower migration barrier than Si but nevertheless has a lower diffusivity. Hence, for a quantitative understanding of the diffusion coefficients, or even a qualitative description of the trends, we find that it is crucial not only to assess the migration barriers and activation energies, but also to understand in detail the underlying factors entering the diffusion pre-factor, including the contribution of the correlation factor.

5. Conclusions

We have illustrated how impurity diffusion coefficients can be predicted directly from first principles without any empirical or fitting parameters. Specifically, we have used DFT static (energy) and dynamic (vibrational) calculations to obtain the correlation factor through a five frequency model, the impurity jump frequency within the framework of transition state theory and the free energies of vacancy formation and vacancy–solute binding. We use our framework to calculate the impurity diffusion coefficients of Mg, Si and Cu in dilute fcc Al alloys. Using our approach we are able to obtain the values of individual diffusion parameters along with the diffusion pre-factor D_o and activation energy Q. The results match well with the experimental data. Both the diffusion pre-factor and the activation energy are key to a quantitative description of solute diffusivities, and we find that even the qualitative trends of diffusivity in Al may not always be inferred from activation energies or migration barriers alone.

Acknowledgments

Work at Penn State was funded by the National Science Foundation (NSF) through Grants DMR-0510180 and DMR-0205232. C.W. acknowledges support from the US

Department of Energy under project DE-FG02-98ER 45721 and the US Automotive Materials Partnership (USAMP) through the US Council for Automotive Research (US-CAR), Contract 07-1876. First principles calculations were carried out on the LION clusters at The Pennsylvania State University supported in part by NSF Grants DMR-9983532 and DMR-0122638 and in part by the Materials Simulation Center and the Graduate Education and Research Services at The Pennsylvania State University.

References

[1] Adams JB. J Mater Res 1989;4:102.
[2] Blochl PE, Smargiassi E, Car R, Laks DB, Andreoni W, Pantelides ST. Phys Rev Lett 1993;70:2435.
[3] Blochl PE, Van de Walle CG, Pantelides ST. Phys Rev Lett 1990;64:1401.
[4] Frank W, Breier U, Elsasser C, Fahnle M. Phys Rev Lett 1996;77:518.
[5] Janotti A, Kremar M, Fu CL, Reed RC. Phys Rev Lett 2004;92:085901.
[6] Krcmar M, Fu CL, Janotti A, Reed RC. Acta Mater 2005;53:2369.
[7] Milman V, Payne MC, Heine V, Needs RJ, Lin JS, Lee MH. Phys Rev Lett 1993;70:2928.
[8] Sandberg N, Magyari-Kope B, Mattsson TR. Phys Rev Lett 2002;89:065901.
[9] Mantina M, Wang Y, Arroyave R, Wolverton C, Chen LQ, Liu ZK. Phys Rev Lett 2008;100:215901.
[10] LeClaire AD, Lidiard AB. Phil Mag 1955;47:518.
[11] Simonovic D, Sluiter MHF. Phys Rev B 2009;79:054304.
[12] Janotti A, Krcmar M, Fu CL, Reed RC. Phys Rev Lett 2004;92:85901.
[13] Lazarus D. Phys Rev 1954;93:973.
[14] Swalin RA. Acta Metall 1957;5:443.
[15] Peterson NL, Rothman S. J. Phys Rev B 1970;1:3264.
[16] Neumann G, Hirschwald W. Phys Status Solidi B 1973;55:99.
[17] Manning JR. Diffusion kinetics for atoms in crystals. Princeton (NJ): D. Van Nostrand; 1968.
[18] Le Claire AD. Correlation effects in diffusion in solids. New York: Academic Press; 1970. p. 261.
[19] Manning JR. Phys Rev 1964;136:A1758.
[20] Wert C, Zener C. Phys Rev 1949;76:1169.
[21] Vineyard GH. J Phys Chem Solids 1957;3:121.
[22] Le Claire AD. J Nucl Mater 1978;69–70:70.
[23] Kresse G, Furthmuller J. Phys Rev B 1996;54:11169.
[24] Kresse G, Joubert D. Phys Rev B 1999;59:1758.
[25] Blochl PE. Phys Rev B 1994;50:17953.
[26] Ceperley DM, Alder BJ. Phys Rev Lett 1980;45:566.
[27] Perdew JP, Burke K, Wang Y. Phys Rev B 1996;54:16533.
[28] Henkelman G, Jonsson H. J Chem Phys 2000;113:9978.
[29] Wei S, Chou MY. Phys Rev Lett 1992;69:2799.
[30] Van de Walle A, Asta M, Ceder G. CALPHAD 2002;26:539.
[31] Mattsson AE, Kohn W. J Chem Phys 2001;115:3441.
[32] Vitos L, Ruban AV, Skriver HL, Kollar J. Surf Sci 1998;411:186.
[33] Carling K, Wahnstrom G, Mattsson TR, Mattsson AE, Sandberg N, Grimvall G. Phys Rev Lett 2000;85:3862.
[34] Mantina M. Materials Science and Engineering. Pennsylvania State University: University Park (PA); 2008. p. 232.
[35] Hillert M. Phase equilibria, phase diagrams and phase transformations: their thermodynamic basis. Cambridge: Cambridge University Press; 1998.
[36] Van de Walle A, Ceder G. Rev Mod Phys 2002;74:11.
[37] Wolverton C. Acta Mater 2007;88:5867.
[38] Balluffi RW, Ho PS. Diffusion. Metals Park (OH): American Society for Metals; 1973. p. 83.
[39] Boisvert G, Lewis LJ, Yelon A. Phys Rev Lett 1995;75:469.
[40] Sandberg N, Holmestad R. Phys Rev B 2006:73.
[41] Wang Y, Curtarolo S, Jiang C, Arroyave R, Wang T, Ceder G, Chen LQ, Liu ZK. CALPHAD 2004;28:79.
[42] Moffatt WG. Handbook of binary phase diagrams. Schenectady (NY): Genium Publishing; 1978.
[43] Fujikawa S-I, Takada Y. Defect Diffus Forum 1997;143–147:409.
[44] Minamino Y, Yamane T, Miyake T, Koizumi M, Miyamoto Y. Mater Sci Technol 1986;2:777.
[45] Rothman SJ, Peterson NL, Nowicki LJ, Robinson LC. Phys Status Solidi B 1974;63:29.
[46] Fujikawa S, Hirano K. Mater Sci Eng 1977;27:25.
[47] Hisayuki K, Yamane T. Z MetalIkd 1999;90:423.
[48] Moreau G, Cornet JA, Calais D. J Nucl Mater 1971;38:197.
[49] Verlinden J, Gijbbels R. Adv Mass Spectrom 1980;8A:485.
[50] Fujikawa S, Hirano K-I, Fukushima Y. Metall Trans A 1978;9:1811.
[51] Beerwald AH. Z Elektrochem Angew Phys Chem 1939;45:789.
[52] Bergner D, Cyrener E. Neue Hutte 1973;18:356.
[53] Mehl RH, Rhines FN, Vonden Steinen KA. Metals and Alloys 1941;13:41.
[54] Fujikawa S, Hirano K. Defect Diff Forum 1989;66–69:453.
[55] Anand MS, Agrawala RP. Phil Mag 1972;26:297.
[56] Murphy JB. Acta Metall 1961;9:563.
[57] Erhart P, Jung P, Schultz H, Ullmaier H. Landolt-Bornstein, New Series, Group III. Berlin: Springer-Verlag; 1991.
[58] Du Y, Chang YA, Huang B, Gong W, Jin Z, Xu H, Yuan Z, Liu Y, He Y, Xie F-Y. Mater Sci Eng 2003;2003:140.